THE JOURNAL OF BIOLOGICAL CHEMISTRY
Vol. 274, No. 37, Issue of September 10, pp. 26172–26178, 1999

Printed in U.S.A.

Horseshoe Crab Hemocyte-derived Antimicrobial Polypeptides, Tachystatins, with Sequence Similarity to Spider Neurotoxins*

(Received for publication, March 16, 1999, and in revised form, May 18, 1999)

Tsukasa Osaki‡, Miyuki Omotezako§, Ranko Nagayama§, Michimasa Hirata¶, Sadaaki Iwanaga§, Jiro Kasahara‡‖, Junji Hattori§, Isao Ito‡§, Hiroyuki Sugiyama‡§, and Shun-ichiro Kawabata‡§**

From the ‡Department of Molecular Biology, Graduate School of Medical Science, Fukuoka 812-8582, the §Department of Biology, Kyushu University, Fukuoka 812-8581, and the ¶Department of Bacteriology, Iwate Medical University, Morioka 020-8505, Japan

Antimicrobial peptides, named tachystatins A, B, and C, were identified from hemocytes of the horseshoe crab *Tachypleus tridentatus*. Tachystatins exhibited a broad spectrum of antimicrobial activity against Gram-negative and Gram-positive bacteria and fungi. Of these tachystatins, tachystatin C was most effective. Tachystatin A is homologous to tachystatin B, but tachystatin C has no significant sequence similarity to tachystatins A and B. Tachystatins A and B showed sequence similarity to ω-agatoxin-IVA of funnel web spider venom, a potent blocker of voltage-dependent calcium channels. However, they exhibited no blocking activity of the P-type calcium channel in rat Purkinje cells. Tachystatin C also showed sequence similarity to several insecticidal neurotoxins of spider venoms. Tachystatins A, B, and C bound significantly to chitin. A causal relationship was observed between chitin binding activity and antifungal activity. Tachystatins caused morphological changes against a budding yeast, and tachystatin C had a strong cell lysis activity. The septum between mother cell and bud, a chitin-rich region, was stained by fluorescence-labeled tachystatin C, suggesting that the primary recognizing substance on the cell wall is chitin. As horseshoe crab is a close relative of the spider, tachystatins and spider neurotoxins may have evolved from a common ancestral peptide, with adaptive functions.

Immunity to infectious agents is mediated by two general systems, innate and acquired. Innate immunity is phylogenetically older than acquired immunity, and a certain form of innate immunity is present in all multicellular organisms. Insects respond to septic injury by the rapid and transient synthesis of defense molecules, as an acute phase reaction (1, 2). On the other hand, major defense molecules of horseshoe crab are constitutively present in hemolymph plasma and hemocytes (3–8). The hemolymph contains granular hemocytes comprising 99% of total hemocytes (9). These granular hemocytes have two populations of secretory granules, named large and small granules (9). These hemocytes are highly sensitive to lipopolysaccharides, which are major outer membrane components of Gram-negative bacteria. The defense molecules stored in both granules are secreted by exocytosis after stimulation with lipopolysaccharides. This response is important for the host defense related to engulfing and killing invading microbes in addition to preventing the leakage of hemolymph. Large granules contain all the clotting factors essential for hemolymph coagulation in addition to various protease inhibitors (10–13) and lectins (14–17). On the other hand, small granules contain mainly antimicrobial substances such as tachyplesin (18) and several cysteine-rich peptides of molecular masses of 6–8 kDa, but functions are unknown (19). Two components of small granules, big defensin and tachycitin, have been functionally and structurally characterized (20, 21).

Horseshoe crab hemocyte-derived antimicrobial peptides named tachystatins A, B, and C, with structural similarity to spider neurotoxins, were newly purified and biochemically characterized. Unlike big defensin and tachycitin previously identified, these tachystatins have a characteristic chitin binding ability in addition to a strong antimicrobial activity against Gram-negative and Gram-positive bacteria and fungi.

EXPERIMENTAL PROCEDURES

Materials—Hemocyte debris from the Japanese horseshoe crab *Tachypleus tridentatus* was prepared as described (22). Tachyplesin (18), big defensin (20), and tachycitin (21) were purified as described. Sources of materials used were as follows; Sephadex G-50 fine and S-Sepharose fast flow from Amersham Pharmacia Biotech, chitin from Seikagaku Corp., Tokyo, wheat germ agglutinin and lysyl endopeptidase from Wako Pure Chemical Industries, Ltd., Tokyo, endoproteinase Asp-N from Roche Molecular Biochemicals, trypsin and chymotrypsin from Worthington Biochemical Co., Freehold, NJ, basal medium Eagle, human transferrin, and bovine insulin from Life Technologies, Inc., bovine serum albumin, aprotinin, L-thyroxin, DNase I, and calcofluor from Sigma, a sheep blood sample from Nippon Bio-Test Laboratories, Tokyo, and ω-agatoxin IVA from Peptide Institute Inc., Osaka.

Antimicrobial Activity and Morphological Effects of Tachystatins on Bacteria and Fungi—Antimicrobial activity was assayed as described (20) using *Escherichia coli* (clinical isolate), *Staphylococcus aureus*, *Candida albicans*, and *Pichia pastoris*. For microscopic analysis, *P. pastoris* was collected by centrifugation and washed twice with 10 mM sodium phosphate buffer, pH 7.0. The fungal suspension, 10 μl, was mixed with 10 μl of a 2-fold serial-diluted tachystatins A, B, or C with the same buffer and placed in each well of a 12-well slide glass and incubated at 30 °C for 2 h. Morphological changes were assessed using an Olympus microscope, model BX 50.

For fluorescence microscopic analysis, tachystatin C was labeled using an Alexa™ 488 protein labeling kit (Molecular Probes, Inc., Eugene, OR) and a protocol provided by the manufacturer. The suspension of *P. pastoris* was mixed with the labeled tachystatin C (a final concentration of 0.18 mg/ml) or the fluorescence ligand coupled with bovine serum albumin (a final concentration of 0.5 mg/ml) as a negative

* This work was supported by a grant-in-aid for scientific research from Ministry of Education, Science, Sports, and Culture of Japan (to S. K.) and CREST (Core Research for Evolutional Science and Technology) of Japan Science and Technology Corporation (to S. K.). The costs of publication of this article were defrayed in part by the payment of page charges. This article must therefore be hereby marked "*advertisement*" in accordance with 18 U.S.C. Section 1734 solely to indicate this fact.

The nucleotide sequence reported in this paper has been submitted to the DDBJ/GenBank™/EBI Data Bank with accession number AB023783.

‖ Present address: Dept. of Pharmacology, Kumamoto University School of Medicine, 2-2-1 Honjo, Kumamoto 860-0811, Japan.

** To whom correspondence should be addressed: Dept. of Biology, Kyushu University, Fukuoka 812-8581, Japan. Tel. and Fax: 81-92-642-2633 or 2634; E-mail: skawascb@mbox.nc. kyushu-u.ac.jp.

control and incubated at 22 °C for 15 min. Under these conditions, tachystatin C caused little cell lysis of *P. pastoris*. A chitin binding fluorescence agent, calcofluor (a final concentration of 0.1 mg/ml) was also used for positive staining of the cell wall. Fluorescence microscopy was done using an Olympus fluorescence microscope, model BX-FLA.

Chitin binding Assay—Chitin (0.5 mg) was mixed with antimicrobial substances in 100 μl of 20 mM Tris-HCl buffer, pH 7.5, containing 0.15 M NaCl and 2 mM $CaCl_2$, then incubated at room temperature for 15 min and centrifuged at 15,000 rpm for 2 min. The supernatant was removed, and the precipitate was washed with 1 ml of the same buffer and eluted with 100 μl of 0.1 M HCl. The concentrations of the bound form were determined using a micro BCA™ protein assay kit from Pierce.

Hemolytic Activity—Antimicrobial substances dissolved in 0.5 ml of 50 mM Tris-HCl, pH 7.5, containing 0.15 M NaCl were mixed with the same volume of sheep erythrocytes in the same buffer (final 1%, v/v) and incubated at 37 °C. An aliquot was taken at a 1-h interval and centrifuged to obtain supernatant. The hemolytic activity was determined by measuring the absorbance at 546 nm as a result of hemoglobin released from erythrocytes and compared with complete lysis (100% hemolysis) obtained by adding deionized water instead of saline.

Proteolytic Digestion—The samples were reduced and *S*-alkylated with 4-vinylpyridine as described (23). The *S*-alkylated tachystatin A was digested with trypsin or chymotrypsin (E/S = 1/25, w/w) in 0.1 M NH_4HCO_3 containing 2 M urea at 37 °C for 12 h. The *S*-alkylated tachystatin B was digested with endoproteinase Asp-N (E/S = 1/25, w/w) in 20 mM Tris-HCl, pH 7.5, containing 2 M urea at 37 °C for 12 h. The *S*-alkylated tachystatin C was digested with lysyl endopeptidase (enzyme/substrate = 1/25, w/w) in 0.1 M NH_4HCO_3 containing 2 M urea at 37 °C for 12 h. The resulting peptides were separated by reverse-phase HPLC[1] using a Cosmosil 5C18 MS (2.0 × 150 mm, Nacalai Tesque Inc., Kyoto) or a μBondasphere 5C8 (2.1 × 150 mm, Waters, Millipore, Milford, MA) column with a linear gradient of 0–48% acetonitrile in 0.06% trifluoroacetic acid for 90 min at a flow rate of 0.2 ml/min. The effluent was monitored at 210 nm.

Amino Acid and Sequence Analyses—Amino acid analysis was performed on a Waters PICO-TAG system. Protein concentrations for determining extinction coefficients of tachystatins were calculated from the amino acid mass/A_{280}. An internal standard, norleucine, was added to the protein hydrolysates to allow for correction for losses. Amino acid sequence analysis was carried out using an Applied Biosystems 477A or 473A gas phase sequencer.

ESI-Mass Spectrometry—The ESI-mass spectrometry spectra were obtained using a JMS-HX/HX110A double-focusing mass spectrometer (JEOL, Tokyo) equipped with an ESI ion source (Analytical of Branford, Branford, CT). Experimental details were as described (24).

Tachystatin A-specific DNA Probe and Screening of cDNA Library—The degenerate nucleotide sequences of the primers used for polymerase chain reaction were based on the amino acid sequences of QGFNCV (residues 7–12) and YFPGST (residues 32–37) of tachystatin A. Sense and antisense nucleotides were synthesized with an *Eco*RI site at the 5′ end. Reactions for polymerase chain reaction contained the cDNA template (corresponding to 0.1 μg of poly(A)$^+$ RNA) and 100 pmol each of the primer was carried out using a Perkin-Elmer thermal cycler. The polymerase chain reaction products were treated with *Eco*RI and purified using agarose gel electrophoresis. Fragments of interest were then ligated into plasmid Bluescript II SK$^+$ (Stratagene, La Jolla, CA) for sequence analysis, as described by Sambrook *et al.* (25). One clone that contained the sequence of tachystatin A was used as a probe. A λZipLox cDNA library was screened by the probe, as described (15). A positive clone with a 0.55-kilobase pair insert was sequenced in both orientations using an Applied Biosystems 373A DNA sequencer, using sequencing primers.

SDS-PAGE—SDS-PAGE was performed according to Laemmli (26). The gels were stained with Coomassie Brilliant Blue R-250.

Homology Search—Computer-assisted homology search was made using the Internet BLAST Search of National Center for Biotechnology Information (NCBI).

Electrophysiology—Cultivation of Purkinje cells and the electrophysiological experiments were done as described (27). Cerebella were dissected from rat fetuses around embryonic days 18 to 20, treated with 1% trypsin, and dispersed in serum-free defined medium (28) by gentle pipetting, then plated on 10-mm round glass coverslips coated with poly-L-lysine. Purkinje cells after the days 25 to 35 *in vitro* were voltage-clamped at −80 mV and depolarized periodically to −10 mV for 60 ms to record Ca^{2+} currents using the whole-cell patch clamp recording system (27). The compositions of external and patch internal solutions were as follows: external solution, 10 mM Hepes-NaOH, pH 7.35, containing 150 mM NaCl, 5 mM KCl, 1 mM $MgCl_2$, 2 mM $CaCl_2$, 10 mM glucose, 0.003 mM tetrodotoxin, 10 mM tetraethylammonium chloride, and 1 mM 4-aminopyridine; patch internal solution, 10 mM Hepes-CsOH, pH 7.35, containing 140 mM CsCl, 1 mM EGTA, 2 mM MgATP, and 0.4 mM NaGTP. ω-Agatoxin IVA and tachystatins A and B were dissolved in deionized water and diluted with external solution just before use.

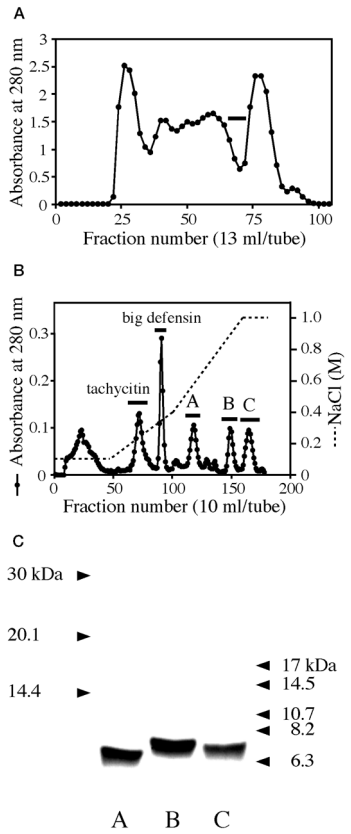

FIG. 1. **Elution profiles for tachystatins from a Sephadex G-50 column and an S-Sepharose column.** *A*, gel filtration of acid extract obtained from the hemocyte debris on a Sephadex G-50 column (3.6 × 110 cm). Fractions indicated by a *solid bar* were collected. *B*, ion exchange column chromatography on an S-Sepharose fast flow column (2 × 32 cm). A *broken line* indicates the concentration of NaCl. *C*, SDS-PAGE of purified tachystatins A, B, and C under reducing conditions.

RESULTS

Purification of Three Types of Tachystatins—The hemocyte debris (36 g, wet weight) was extracted twice by homogenizing with 200 ml of 30% acetic acid, and the supernatant obtained by centrifugation at 14,000 rpm for 15 min was lyophilized. The dried material was dissolved in 50 ml of 10% acetic acid and applied to a Sephadex G-50 column (3.6 × 110 cm) equilibrated with 10% acetic acid (Fig. 1*A*). SDS-PAGE in a 15% gel of every two tubes indicated the presence of peptides within molecular masses of 6 to 8 kDa in fractions 66–72 (data not shown). These fractions were collected, lyophilized, and then applied to an S-Sepharose fast flow column (2 × 32 cm) equilibrated with 20 mM Tris-HCl, pH 8.0, containing 0.1 M NaCl. After washing with the equilibration buffer, peptides were eluted with two steps of a linear NaCl gradient of 0.1 to 0.4 M and then 0.4 to 1.0 M in the same buffer (Fig. 1*B*). Two separated peaks were eluted with the first gradient, and both peaks contained an 8-kDa peptide on SDS-PAGE (data not shown). The partial NH_2-terminal sequence analysis revealed that the first and second peaks contained the previously characterized antimicro-

[1] The abbreviations used are: HPLC, high performance liquid chromatography; ESI, electrospray ionization; PAGE, polyacrylamide gel electrophoresis.

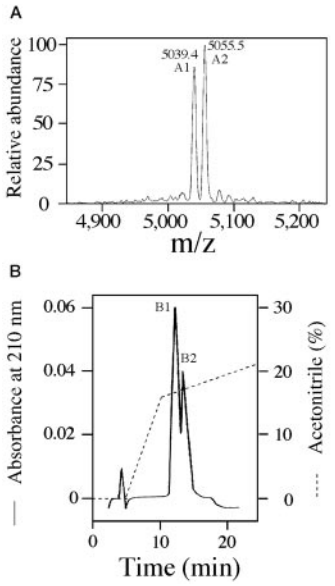

FIG. 2. **Isopeptides of tachystatins A and B.** *A*, ESI-mass spectrometry of tachystatin A. *B*, separation of tachystatins B1 and B2 by HPLC. Tachystatin B was applied to a phenyl-5PW reverse-phase column (4.6 × 75 mm) and eluted at a flow rate of 0.5 ml/min with a linear gradient of acetonitrile containing 0.06% trifluoroacetic acid.

bial substances, tachycitin (21) and big defensin (20), respectively. The second step of the NaCl gradient yielded three separated peaks (A, B, and C in Fig. 1*B*), and each contained peptides of 6.8, 7.4, and 7.1-kDa on SDS-PAGE, respectively (Fig. 1*C*). These peptides had antimicrobial activity and were named tachystatin A, tachystatin B, and tachystatin C, respectively.

The NH_2-terminal sequence analysis for tachystatin A showed a sequence of YSR*X* without contamination. However, the ESI-mass spectrometry gave two peaks at m/z = 5039.4 and 5055.5 (Fig. 2*A*), indicating the presence of the two isoforms, named tachystatin A1 and tachystatin A2, respectively. The two isoforms, however, could not be separated by reverse-phase HPLC. The NH_2-terminal sequence of Y(V/I)(S/T)*X*L for tachystatin B was determined with the ratio of Val:Ile at the second cycle of 5.9:4.1. Tachystatin B could be partially separated into two peaks by reverse-phase HPLC, named tachystatin B1 and tachystatin B2 (Fig. 2*B*). Based on their peak heights, tachystatins B1 and B2 were present at the ration of 6:4. By sequencing of the two peptides, Val-Ser and Ile-Thr at the second and third positions were identified for tachystatin B1 and for tachystatin B2, respectively. For tachystatin C, the NH_2-terminal sequence of DYDWS was determined, and no isoforms were found.

All of the antimicrobial components so far identified in small granules of the horseshoe crab hemocytes have a characteristic chitin binding activity (21). The three types of tachystatins isolated here also bound to chitin and could be eluted by 10% acetic acid and then lyophilized. The extinction coefficients of tachystatins at 280 nm for a 1% solution in deionized water were calculated from the data on amino acid analyses. The values of 18.5 for tachystatin A, 15.2 for tachystatin B, and 51.8 for tachystatin C were used to estimate the peptide concentrations. The yields from 100 g of hemocyte debris were 6.0 mg for tachystatin A, 7.0 mg for tachystatin B, and 1.4 mg for tachystatin C. The isopeptides of tachystatins A and B could not be completely separated by reverse-phase HPLC, and the lyophilized samples, after desalting by the chitin-column chromatography, were used for subsequent assays. No significant contamination other than the isopeptides in these samples was confirmed by amino acid analysis (see Table III).

TABLE I
Antimicrobial activities of the horseshoe crab chitin binding peptides

Amino acid residues		pI[a]	IC_{50}[b]			
			E. coli	*S. aureus*	*C. albicans*	*P. pastoris*
			$\mu g/ml$			
Tachystatin A	44	11.8	25	4.2	3.0	0.5
Tachystatin B	42	12.0	NI[c]	7.4	3.0	0.1
Tachystatin C	41	11.9	1.2	0.8	0.9	0.3
Tachyplesin	17	12.3	<2.5	0.3	0.2	0.1
Big defensin	79	10.6	2.5	<2.5	20	42
Tachycitin	73	10.1	33	56	52	41

[a] Each pI value of the peptides was calculated from the amino acid compositions (46).
[b] 50% growth inhibitory concentration.
[c] No inhibition at 100 μg/ml.

Antimicrobial Activity and Morphological Effects of Tachystatins on Bacteria and Fungi—The 50% inhibitory concentrations (IC_{50}) of tachystatins for growth of various bacteria and fungi were determined, as summarized in Table I. Tachystatins A and B exhibited stronger antimicrobial activity against the Gram-positive bacteria (*S. aureus*) and fungi (*C. albicans* and *P. pastoris*) than Gram-negative bacteria (*E. coli*). Tachystatin B was inactive against *E. coli* up to 100 μg/ml. In contrast, tachystatin C showed strong activity against *E. coli* with an IC_{50} value of 1.2 μg/ml. Tachystatin C was also very active against *S. aureus, C. albicans*, and *P. pastoris*, with the equivalent potency of IC_{50} values.

Morphological changes of fungi by tachystatins were observed using a budding yeast *P. pastoris* (Fig. 3). In the presence of tachystatin C at 0.1 μg/ml, one-third of IC_{50}, *P. pastoris* shrank, and the diameter was reduced to about one-half (Fig. 3, *A* and *B*). At 3 μg/ml, a 10-fold higher concentration of IC_{50}, tachystatin C clearly caused cell lysis (Fig. 3*C*).

Chitin Binding Activity of Tachystatins—To compare quantitatively the chitin binding ability, different amounts of the horseshoe crab antimicrobial components were mixed with the constant amount of chitin, and the amounts bound were quantitated. Chitin binding activity was expressed, as the half-maximum concentration required for reaching a plateau of chitin binding. A progression curve of tachystatin C bound to chitin is shown in Fig. 4, and parameters of the chitin binding activities are summarized in Table II. The three tachystatins bound to chitin at the half-maximum concentrations of 4.3–8.4 μM, equivalent to those obtained for tachyplesin and a plant chitin binding lectin, wheat germ agglutinin (29, 30). These data indicate that tachystatins also belong to the family of chitin binding antimicrobial substances.

Visualization of Chitin Binding Activity—The broad spectrum of antimicrobial activity and chitin binding activity of tachystatins suggested that tachystatins recognize bacterial cell wall components. The cell wall of budding yeasts contains several polysaccharides, such as mannan, glucan, and chitin. During budding in the cell cycle, chitin has been identified mainly in a primary septum at the constriction between mother cell and budding daughter cell (31). This region can be visualized by a fluorescent brightener, calcofluor (32, 33). When *P. pastoris* was treated with calcofluor, the septum region between mother cell and bud was clearly stained (Fig. 5*B*). To visualize tachystatins bound to the cell wall, tachystatin C was fluorescence labeled by Alexa 488. The labeled tachystatin C was mixed with *P. pastoris*, and photomicroscopy was done as described under "Experimental Procedures." The labeled tachystatin C was localized at the *P. pastoris* envelope and seems to be concentrated at the septum region (Fig. 5*A*). The cell wall was not stained by fluorescence-labeled bovine serum albumin, used as a control (data not shown).

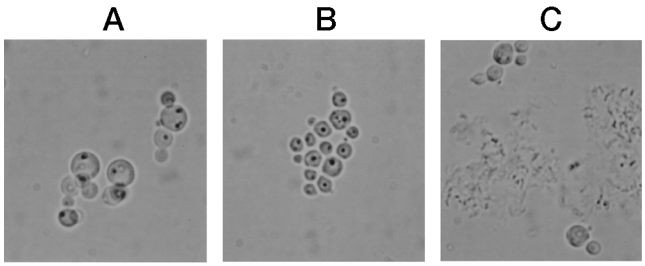

FIG. 3. **Morphological changes of *P. pastoris* treated with tachystatin C.** Experimental details are described under " Experimental Procedures." *A*, nontreated *P. pastoris*. *B*, *P. pastoris* treated with 0.1 μg/ml tachystatin C. *C*, *P. pastoris* treated with 3 μg/ml tachystatin C. Magnification: ×1,000.

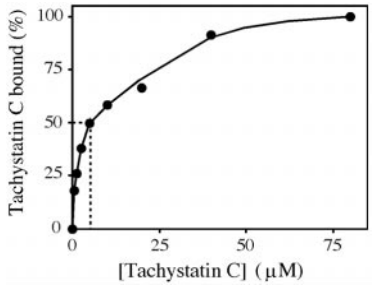

FIG. 4. **Chitin binding activity of tachystatin C.** Chitin was mixed with the indicated amount of tachystatin C and incubated at room temperature for 15 min. The amount of protein bound was measured as described under "Experimental Procedures."

TABLE II
Chitin binding activities of the horseshoe crab antimicrobial peptides

	Concentration required for 50% binding
	μM
Tachystatin A	8.4
Tachystatin B	4.3
Tachystatin C	5.2
Tachyplesin	6.6
Big defensin	25.4
Tachycitin	19.5
Wheat germ agglutinin[a]	9.0

[a] Wheat germ agglutinin was calculated as the dimer (M_r, 37,510).

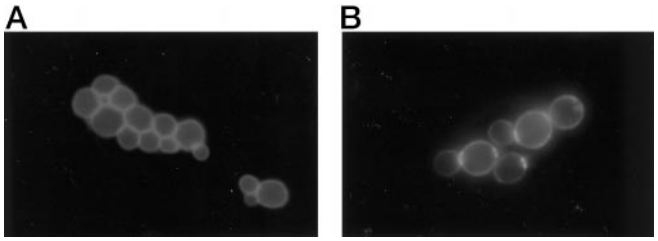

FIG. 5. **Fluorescence of *P. pastoris* treated with the fluorescence-labeled tachystatin C.** Experimental details are presented under "Experimental Procedures." *A*, *P. pastoris* treated with the fluorescence-labeled tachystatin C. *B*, *P. pastoris* treated with calcofluor. Magnification: ×1,000.

Hemolytic Activity of Tachystatins—Because tachystatin C could lyse *P. pastoris* cells, effects of three types of tachystatins on sheep erythrocytes were investigated and compared with findings in other horseshoe crab antimicrobial substances. Tachystatin C caused hemolysis in time- and dose-dependent manners, but tachystatins A and B and the antimicrobial substances, including tachyplesin, big defensin, and tachycitin, had little or no effect on the erythrocytes under the same conditions (Figs. 6, *A* and *B*). Several hemolysins and hemolytic lectins form ion-permeable pores in erythrocyte membranes, and their hemolytic activities are protected by the addition of

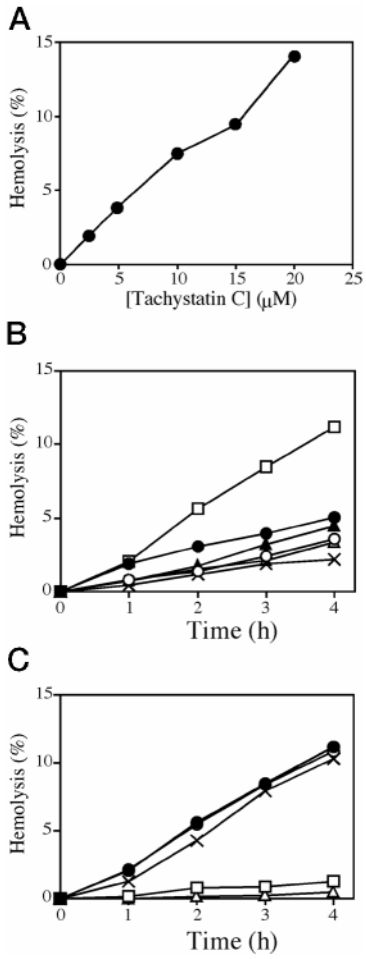

FIG. 6. **Hemolytic activity of tachystatin C.** *A*, increasing amounts of tachystatin C (2.5 to 20 μM) were mixed with sheep erythrocytes and incubated for 4 h at 37 °C. Hemolytic activity was assayed, as described under "Experimental Procedures." *B*, hemolytic activity of various antimicrobial peptides (10 μM) derived from horseshoe crab hemocytes; tachyplesin (●), big defensin (○), tachycitin (X), tachystatin A (△), tachystatin B (▲), and tachystatin C (□). *C*, osmotic protection assays against hemolysis by several polyethylene glycols or dextran 4. The hemolysis of sheep erythrocytes was measured in the absence (●) or the presence of polyethylene glycols (30 mM): polyethylene glycol 600 (○), polyethylene glycol 1,540 (X), and polyethylene glycol 4,000 (□), or dextran 4 (△) (30 mM). Measurements were made in duplicate with 10 μM of tachystatin C.

polyethylene glycols or dextrans, an osmotic protection (34). To test whether or not the hemolytic activity of tachystatin C is due to the formation of ion-permeable pores on the plasma membranes, osmotic protection assay was done. Sheep erythrocytes were incubated with tachystatin C in the presence of several protectants with different molecular sizes. The hemolysis was inhibited strongly as the molecular sizes of polyethylene glycols or dextrans increased; polyethylene glycol 600 (molecular diameter = 1.6 nm) and polyethylene glycol 1540 (2.4 nm) afforded little or no protection against lysis, whereas dextran 4 (3.5 nm) and polyethylene glycol 4000 (3.8 nm) gave 88 and 95% protection against hemolysis, respectively (Fig. 6*C*). These results indicate the presence of ion-permeable pores on the erythrocyte membranes with a diameter of about 3.5 nm.

Peptide and Nucleotide Sequencing of Three Types of Tachystatins—The amino acid sequences of tachystatins A1, A2, B1, B2, and C were determined by NH_2-terminal sequence analyses of the *S*-pyridylethylated tachystatins and their peptide fragments produced by proteolytic digests (Fig. 7). Tachystatins A1 and A2 could not be separated by reverse-phase

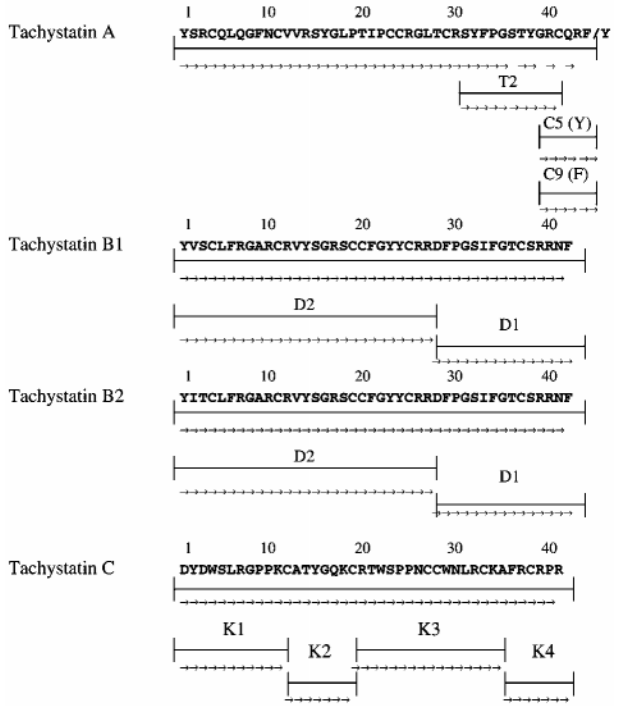

FIG. 7. **Amino acid sequences of tachystatins.** Residues identified using a gas phase sequencer are indicated by *arrows*. *T*, trypsin-digested peptides; *C*, chymotrypsin-digested peptides; *D*, endoproteinase Asp N-digested peptides; *K*, lysyl endopeptidase-digested peptides.

TABLE III
Amino acid compositions of tachystatins A, B, and C
Compositions are calculated from 20-h hydrolysates.

Amino acid	Tachystatin A			Tachystatin B			Tachystatin C	
	Analysis	Sequence		Analysis	Sequence		Analysis	Sequence
		A1	A2		B1	B2		
	Residues/molecule			*Residues/molecule*			*Residues/molecule*	
Asp	1.3	(1)	(1)	2.1	(2)	(2)	3.1	(4)
Glu	3.0	(3)	(3)				1.5	(1)
Ser	3.0	(4)	(4)	3.6	(5)	(4)	1.8	(2)
Gly	5.1	(5)	(5)	5.0	(5)	(5)	3.5	(2)
Arg	6.0	(6)	(6)	7.5	(8)	(8)	5.5	(6)
Thr	2.5	(3)	(3)	1.5	(1)	(2)	1.9	(2)
Ala				1.1	(1)	(1)	2.3	(2)
Pro	3.4	(3)	(3)	1.1	(1)	(1)	5.2	(5)
Tyr	4.3	(4)	(5)	4.0	(4)	(4)	1.8	(2)
Val	1.9	(2)	(2)	1.7	(2)	(1)		
Cys	6.5[a]	(6)	(6)	5.9[b]	(6)	(6)	6.0[a]	(6)
Ile	1.0	(1)	(1)	1.5	(1)	(2)		
Leu	3.0	(3)	(3)	0.9	(1)	(1)	2.0	(2)
Phe	2.4	(3)	(2)	5.1	(5)	(5)	0.8	(1)
Trp							ND[c]	(3)
Lys							2.7	(3)
Total		(44)	(44)		(42)	(42)		(41)

[a] Determined as cysteic acid after performic acid oxidation.
[b] Determined as pyridlethyl cysteine.
[c] Not determined.

```
1       10        20        30        40        50        60
CACATTTCAAGCACACAGAATCTGAATAAATAGAAGAGAGAACAGTGTGACGTCATGAAA
                                                M  K

        70        80        90        100       110       120
TTGCAAAATACACTGATTCTGATTGGTTGTCTTTTCTTAATGGGTGCAATGATAGGAGAC
L  Q  N  T  L  I  L  I  G  C  L  F  L  M  G  A  M  I  G  D

        130       140       150       160       170       180
GCATATAGTCGTTGTCAGTTACAAGGATTCAATTGTGTTGTTCGCAGTTATGGATTGCCA
A  Y  S  R  C  Q  L  Q  G  F  N  C  V  V  R  S  Y  G  L  P

        190       200       210       220       230       240
ACTATACCGTGTTGTAGGGGTTTGACATGTCGTTCATACTTTCCAGGATCTACATATGGG
T  I  P  C  C  R  G  L  T  C  R  S  Y  F  P  G  S  T  Y  G

        250       260       270       280       290       300
AGATGCCAAAGATACTGAGAGTAATCCCATCTGACAGTGGTCCTGAGGAAGCTACTGCTT
R  C  Q  R  Y  *

        310       320       330       340       350       360
TAAGATCACTGCAAAAATACATTATTATTGTGCAGTTATCTTTCGATTGCTCTTCTGTTC

        370       380       390       400       410       420
CTTCAGTATTCTATAAATTAATATTTTAATTTAAATAACAGTCTTAAAGAAGACATAGTT

        430       440       450       460       470       480
AAGAAGCTATTAAACTATAAGAAGGAAACAATGTACTAGATGTGAACTCTGTATAACCGT

        490       500       510       520       530       540
TAAAACATTAAATTGTCCCTTTTCTCTGAAAAAAAAAAAAAAAAAAAAAAAAAAAAAAA

  545
AAAAA
```

FIG. 8. **Nucleotide sequence of tachystatin A2.** An *underline* represents the amino acid sequence determined by peptide sequencing of the tachystatin A2. A *star* represents a stop signal.

HPLC, but the amino acid sequence analysis of tachystatin A containing A1 and A2 established the first 42 residues, indicating the amino acid difference between the isoform is located at the COOH-terminal region. Furthermore, the chymotryptic digest of tachystatin A yielded two kinds of the COOH-terminal peptides, C9F containing Phe at the COOH terminus and C5Y containing Tyr at the COOH terminus, indicating that two peptides are derived from tachystatin A1 and tachystatin A2, respectively. The theoretical masses of tachystatins A1 (5039.8) and A2 (5055.8) from the primary structures were consistent with those obtained by ESI-mass spectrometry (Fig. 2*A*). Amino acid analyses indicated that the compositions of the tachystatins A, B, and C were closely consistent with the sum of their sequences (Table III).

A nucleotide sequence was also determined to obtain information on a precursor form of tachystatins, using a probe for tachystatin A as described under "Experimental Procedures." A positive clone with the longest insert was sequenced. The cDNA contained 545 base pairs starting with the ATG codon for an initiation Met at nucleotide position 55 and the stop codon at position 256 followed by a poly(A) tail at position 509 (Fig. 8). An open reading frame coded for an NH_2-terminal signal sequence of 23 residues and a mature tachystatin A2. The precursor contained no propeptide with an Arg-Xaa-Lys/Arg-Arg motif at the cleavage site found in big defensin (35). Moreover, there was no COOH-terminal extension peptides found in tachyplesin (36) and tachycitin (21).

Sequence Similarity—Tachystatin A1 and A2 had 42% sequence identity with tachystatin B1 and B2, respectively (Fig. 9*A*). Tachystatin C, however, exhibited no significant sequence similarity to tachystatins A and B. Homology search revealed interesting sequence identity (22%) of tachystatins A and B with ω-agatoxin-IVA (Fig. 9*A*). ω-Agatoxin-IVA, a neurotoxin isolated from the venom of the funnel web spider (*Agelenopsis aperta*), is a potent blocker of voltage-dependent P-type Ca^{2+} channels in mammals (37). On the other hand, tachystatin C had 30–33% sequence identity to insecticidal peptides isolated from spider venoms, such as μ-agatoxin II from *A. aperta* (38), aptotoxin VII from *Aptostichus schlingeri* (39), and curtatoxins II and III from *Hololena curta* (40) (Fig. 9*B*). μ-Agatoxin II is a neurotoxin that modifies the kinetics of voltage-dependent Na^+ channels in insects (41).

Effects of Tachystatins on Ca^{2+} Channel Currents—To determine if tachystatins block Ca^{2+} channel activity, voltage clamp recording was done using cultured rat cerebellar Purkinje cells. Depolarization of the Purkinje cells resulted in the inward currents (data not shown). When the external solution replaced the Ca^{2+}-free solution, the currents completely disappeared, and these currents were also blocked almost completely with 75 nM ω-agatoxin IVA. The relative amplitudes were 0% ± 0%

A

```
Tachystatin A1  :YSRCQLQGF-NCVVRSYGLPTIPCCRGLTCRSYFPGSTYGRCQRF
Tachystatin B1  :YVSCLFRGA-RCRVYSGRS----CCFGYYCRRDFPGSIFGTCSRRNF
ω-Agatoxin IVA  :KKKCIAKDYGRCKWGGT-----PCCRGRGCICSIMGTNCE-CKPRLIMEGLGLA
```

B

```
Tachystatin C   :DYDWSLRGPPKCATYGQKCRTWSPPNCCWNLRCK-----AFRCRPR
μ-Agatoxin II   :          ECATKNKRCADWAGPWCCDGLYCSCRSYPGCMCRPSS
Aptotoxin VII   :        WLGCARVKEACGPWEWP-CCSGLKCD-----GSECHPQ
Curtatoxin II   :          ADCVGDGQRCADWAGPYCCSGYYCSCRSMPYCRCRSDS
Curtatoxin III  :          ADCVGDGQKCADWFGPYCCSGYYCSCRSMPYCRCRSDS
```

FIG. 9. **Sequence comparisons of tachystatins and neurotoxins from spider venoms.** Consensus amino acid residues are indicated in *bold small capital letters*. The conserved cysteine residues are indicated in *bold large capital letters*. *A*, alignment of the amino acid sequence of tachystatin A1 and B1 with ω-agatoxin-IVA. *B*, alignment of the amino acid sequence of tachystatin C with those of insecticidal peptides from venom of the spiders.

(mean ± S.E.) by Ca^{2+}-free solution and 5% ± 3.5% by 75 nM ω-agatoxin IVA, respectively. These results clearly indicate that the currents are P-type Ca^{2+} currents. In contrast, tachystatins A and B had no apparent effects on P-type Ca^{2+} currents. Relative amplitudes were 96% ± 2.4% by 100 nM tachystatin B and 95% ± 2.2% by 300 nM tachystatin A.

DISCUSSION

Antimicrobial peptides named tachystatins A, B, and C were newly identified from hemocytes of the Japanese horseshoe crab *T. tridentatus*. Furthermore, their isoforms with amino acid replacements for tachystatins A, tachystatins A1 and A2, tachystatin B, and tachystatins B1 and B2 were identified. Tachystatins A (A1 and A2), B (B1 and B2), and C consist of a total 44, 42, and 41 amino acid residues, respectively. The sequence identity between tachystatins A and B is 40%. Tachystatin C showed no significant sequence similarity to tachystatins A and B.

A homology search revealed that tachystatins A and B show sequence similarity to ω-agatoxin-IVA of funnel web spider (*A. aperta*) venom, a potent blocker of voltage-dependent calcium channels. Tachystatin C also shows sequence similarity to those of insecticidal neurotoxins isolated from spider venoms, μ-agatoxin, aptotoxin VII, and curtatoxins II and III. However, tachystatins A and B exhibited no blocking activity of the P-type calcium channel in rat Purkinje neuron. Kim *et al*. (42) reported that the removal of eight amino acid residues from the COOH-terminal region of ω-agatoxin IVA led to a marked reduction in channel-blocking activity, thereby indicating the importance of this region for expressing channel-blocking activity. The hydrophobic COOH-terminal extension found in ω-agatoxin IVA is missing from the sequences of tachystatins, and this may explain the lack of blocking activity of tachystatins for the ion channel. Antimicrobial peptides from scorpion blood also have sequence similarity to several neurotoxins, which are ion channel blockers (43). The horseshoe crab is a close relative of spiders and scorpions, all of which belong to Chelicerata. Therefore, these tachystatins and spider neurotoxins may have evolved from a common ancestral peptide, with adaptive functions.

Tachystatin C but not tachystatins A and B exhibits hemolytic activity. Moreover, osmotic protection assays suggest that tachystatin C forms ion-permeable pores with a diameter of about 3.5 nm on the membranes (Fig. 6). Several proteins and peptides with cytolytic properties possess a common sequence feature of a cationic site flanked by a hydrophobic surface (44). ω-Agatoxin IVA (42) and μ-agatoxin (45) consist of a triple-stranded β-sheet. If the three kinds of tachystatins have a common structural motif, the COOH-terminal part of tachystatin C appears to form an amphiphilic β-sheet, but the corresponding β-sheets of tachystatins A and B do not have the amphiphilic character (Fig. 10). Therefore, the amphiphilic COOH-terminal region of tachystatin C may have an important role in hemolytic activity and cell lysis of *P. pastoris*.

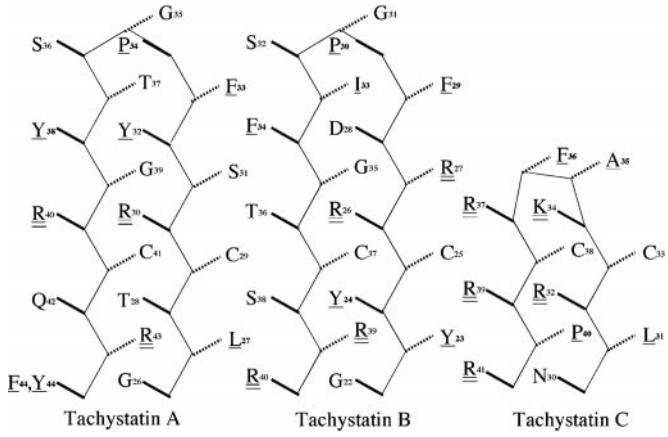

FIG. 10. **β-Sheet structural models of the COOH-terminal regions of tachystatins A, B, and C.** *Solid/dashed lines* indicate side chains pointing out of/into the plane of the diagram. Basic and hydrophobic amino acid residues are indicated in *double underlines* and *single underlines*, respectively.

Tachystatins have a broad spectrum of antimicrobial activity against Gram-negative and Gram-positive bacteria and fungi. Among them, tachystatin C is the most effective with the same potency against these microorganisms (Table I). Tachystatins, therefore, could recognize different types of cell wall components, such as lipopolysaccharides of Gram-negative bacteria, lipoteichoic acids of Gram-positive bacteria, in addition to mannan, β-glucan, or chitin of fungi. Cell wall binding activity of tachystatin C was visualized on a budding yeast *P. pastoris* using the fluorescence-labeled tachystatin C. The septum region between mother cell and bud, a chitin-rich site of the yeast, was strongly stained. Thus, the primary recognizing substance on the cell wall of fungi is likely to be chitin. Based on these results, there appears to be a causal relationship between chitin binding activity and antifungal activity, since big defensin and tachycitin with lower chitin binding affinity have one or two orders higher IC_{50} values for fungi than those of tachystatins and tachyplesin with higher chitin binding activity (Tables I and II).

Interestingly, the small granule-derived antimicrobial substances so far identified, including tachyplesin, big defensin, tachycitin (21), and tachystatin A, all bind to chitin. On the other hand, horseshoe crab lectins found in the large granules of hemocytes, named tachylectins 1–4, have no apparent binding ability to chitin (data not shown). Thus, the chitin binding property may be a common feature of the small granular components. Chitin is a component of the cell wall of fungi, and it is also the major structural component of arthropod exoskeletons. The antimicrobial substances released from hemocytes probably recognize chitin exposed at the site of a lesion, and they appear to serve not only as antibacterial defense molecules against invading microbes but also in wound healing, which may stimulate and accelerate biosynthesis of chitin at sites of injury.

Acknowledgments—We express our thanks to Drs. T. Takao and Y. Shimonishi (the Institute for Protein Research, Osaka University) for mass analysis, W. Kamada for technical assistance with peptide sequencing and amino acid analyses, and M. Ohara for helpful comments on this manuscript.

REFERENCES

1. Hoffmann, J. A., Hetru, C., and Reichhart, J-M. (1993) *FEBS Lett.* **325,** 63–66
2. Hultmark, D. (1993) *Trends Genet.* **9,** 178–183
3. Iwanaga, S., Miyata, T., Tokunaga, F., and Muta, T. (1992) *Thromb. Res.* **68,**

1–32
4. Iwanaga, S. (1993) *Curr. Opin. Immunol.* **5,** 74–82
5. Muta, T., and Iwanaga, S. (1996) in *Progress in Molecular and Subcellular Biology Invertebrate Immunology* (Rinkevich, B., and Müller, W. E. G., eds) Vol. 15, pp. 154–189, Springer-Verlag, Berlin
6. Muta, T., and Iwanaga, S. (1996) *Curr. Opin. Immunol.* **8,** 41–47
7. Kawabata, S., Muta, T., and Iwanaga, S. (1996) in *New Directions in Invertebrate Immunology* (Söderhäll, K., Iwanaga, S., and Vasta, G. R., eds) pp. 255–284, SOS Publications, Fair Haven, NJ
8. Iwanaga, S., Kawabata, S., and Muta, T. (1998) *J. Biochem.* (*Tokyo*) **123,** 1–15
9. Toh, Y., Mizutani, A., Tokunaga, F., Muta, T., and Iwanaga, S. (1991) *Cell Tissue Res.* **266,** 137–147
10. Nakamura, T., Hirai, T., Tokunaga, F., Kawabata, S., and Iwanaga, S. (1987) *J. Biochem.* (*Tokyo*) **101,** 1297–1306
11. Miura, Y., Kawabata, S., and Iwanaga, S. (1994) *J. Biol. Chem.* **269,** 542–547
12. Miura, Y., Kawabata, S., Wakamiya, Y., Nakamura, T., and Iwanaga, S. (1995) *J. Biol. Chem.* **270,** 558–565
13. Lal Agarwala, K., Kawabata, S., Hirata, M., Miyagi, M., Tsunasawa, S., and Iwanaga, S. (1996) *J. Biochem.* (*Tokyo*) **119,** 85–94
14. Saito, T., Kawabata, S., Hirata, M., and Iwanaga, S. (1995) *J. Biol. Chem.* **270,** 14493–14499
15. Okino, N., Kawabata, S., Saito, T., Hirata, M., Takagi, T., and Iwanaga, S. (1995) *J. Biol. Chem.* **270,** 31008–31015
16. Saito, T., Hatada, M., Iwanaga, S., and Kawabata, S. (1997) *J. Biol. Chem.* **272,** 30703–30708
17. Inamori, K., Saito, T., Iwaki, D., Nagira, T., Iwanaga, S., Arisaka, F., and Kawabata, S. (1999) *J. Biol. Chem.* **274,** 3272–3278
18. Nakamura, T., Furunaka, H., Miyata, T., Tokunaga, F., Muta, T., Iwanaga, S., Niwa, M., Takao, T., and Shimonishi, Y. (1988) *J. Biol. Chem.* **263,** 16709–16713
19. Shigenaga, T., Takayenoki, Y., Kawasaki, S., Seki, N., Muta, T., Toh, Y., Ito, A., and Iwanaga, S. (1993) *J. Biochem.* (*Tokyo*) **114,** 307–316
20. Saito, T., Kawabata, S., Shigenaga, T., Takayenoki, Y., Cho, J., Nakajima, H., Hirata, M., and Iwanaga, S. (1995) *J. Biochem.* (*Tokyo*) **117,** 1131–1137
21. Kawabata, S., Nagayama, R., Hirata, M., Shigenaga, T., Lal Agarwala, K., Saito, T., Cho, J., Nakajima, H., Takagi, T., and Iwanaga, S. (1996) *J. Biochem.* (*Tokyo*) **120,** 1253–1260
22. Nakamura, T., Morita, T., and Iwanaga, S. (1985) *J. Biochem.* (*Tokyo*) **97,** 1561–1574
23. Charbonneau, H. (1989) in *A Practical Guide to Protein and Peptide Purification for Microsequencing* (Matsudaira, P. T., ed) pp. 15–30, Academic Press Inc., San Diego, CA
24. Shimizu, T., Takao, T., Hozumi, K., Nunomura, K., Ohta, S., Shimonishi, Y., and Ikegami, S. (1997) *Biochemistry* **36,** 12071–12079
25. Sambrook, J., Fritsch, E. F., and Maniatis, T. (1989) *Molecular Cloning: A Laboratory Manual*, 2nd Ed., Cold Spring Harbor Laboratory, Cold Spring Harbor, NY
26. Laemmli, U. K. (1970) *Nature* **227,** 680–685
27. Kasahara, J., and Sugiyama, H. (1998) *Neurosci. Lett.* **247,** 139–142
28. Fischer, G. (1982) *Neurosci. Lett.* **28,** 325–329
29. Lotan, R., and Sharon, N. (1973) *Biochem. Biophys. Res. Commun.* **55,** 1340–1346
30. Privat, J. P., Delmotte, F., Mialonier, G., Bouchard, P., and Monsigny, M. (1974) *Eur. J. Biochem.* **47,** 5–14
31. Cabib, E., and Roberts, R. (1982) *Annu. Rev. Biochem.* **51,** 763–793
32. Elorza, M. V., Rico, H., and Sentandreu, R. (1983) *J. Gen. Microbiol.* **129,** 1577–1582
33. Roncero, C., and Durán, A. (1985) *J. Bacteriol.* **163,** 1180–1185
34. Scherrer, R., and Gerhardt, P. (1971) *J. Bacteriol.* **107,** 718–735
35. Kawabata, S., Saito, T., Saeki, K., Okino, N., Mizutani, A., Toh, Y., and Iwanaga, S. (1997) *Biol. Chem.* **378,** 289–292
36. Shigenaga, T., Muta, T., Toh, Y., Tokunaga, F., and Iwanaga, S. (1990) *J. Biol. Chem.* **265,** 21350–21354
37. Mintz, I. M., Venema, V. J., Swiderek, K. M., Lee, T. D., Bean, B. P., and Adams, M. E. (1992) *Nature* **355,** 827–829
38. Skinner, W. S., Adams, M. E., Quistad, G. B., Kataoka, H., Cesarin, B. J., Enderlin, F. E., and Schooley, D. A. (1989) *J. Biol. Chem.* **264,** 2150–2155
39. Skinner, W. S., Dennis, P. A., Li, J. P., and Quistad, G. B. (1992) *Toxicon* **30,** 1043–1050
40. Stapleton, A., Blankenship, D. T., Ackermann, B. L., Chen, T. M., Gorder, G. W., Manley, G. D., Palfreyman, M. G., Coutant, J. E., and Cardin, A. D. (1990) *J. Biol. Chem.* **265,** 2054–2059
41. Adams, M. E., Herold, E. E., and Venema, V. J. (1989) *J. Comp. Physiol. A Sens. Neural. Behav. Physiol.* **164,** 333–342
42. Kim, J. I., Konishi, S., Iwai, H., Kohno, T., Gouda, H., Shimada, I., Sato, K., and Arata, Y. (1995) *J. Mol. Biol.* **250,** 659–671
43. Ehret-Sabatier, L., Loew, D., Goyffon, M., Fehlbaum, P., Hoffmann, J. A., Van Dorsselaer, A., and Bulet, P. (1996) *J. Biol. Chem.* **271,** 29537–29544
44. Kini, R. M., and Herbert, J. E. (1989) *Int. J. Pept. Protein Res.* **34,** 277–286
45. Omecinsky, D. O., Holub, K. E., Adams, M. E., and Reily, M. D. (1996) *Biochemistry* **35,** 2836–2844
46. Skoog, B, and Wichman A. (1986) *Trends Anal. Chem.* **5,** 82–83